miRNAs and their targets regulate plant architecture in *Brassica napus*

Li Chen, Jing Wen, Bin Yi, Chaozhi Ma, Jinxing Tu, Tingdong Fu and Jinxiong Shen*

National Key Laboratory of Crop Genetic Improvement, National Engineering Research Center of Rapeseed, Huazhong Agricultural University, Wuhan 430070, China

* To whom correspondence should be addressed: jxshen@mail.hzau.edu.cn

Abstract

MicroRNAs (miRNAs), a class of non-coding small RNAs, are crucial to the regulation of various developmental processes. Plant architecture, defined as the three-dimensional organization of the plant body, is a collection of genetically controlled agronomic traits that determine crop production and harvest index. Although several genes had been found to regulate plant architecture, the mechanisms whereby miRNAs regulate plant architecture in the rapeseed (*Brassica napus*) remain unknown.

In this study, we characterized a rod-like rapeseed mutant with a dwarf and compact plant architecture that substantially enhanced its breeding potential. To explore miRNAs that contribute to the rapeseed plant architecture, backcross progenies that developed into small plants (rod-like) and tall plants (normal) used for study. Four small RNA (sRNA) libraries and two degradome libraries from the shoot apex of normal and rod-like plants were sequenced. A total of 925 non-redundant *B. napus* miRNA precursors were identified, representing 315 precursors for 74 known miRNAs and 610 precursors for 327 novel miRNAs. Expression analysis revealed that 10 known miRNAs and 7 novel miRNAs were differentially expressed between the normal and rod-like plants. In addition, 408 targets were identified through degradome sequencing and 14 targets were further validated via RNA ligase-mediated 5′ rapid amplification of cDNA ends. Furthermore, the functions of miR319 and its target gene *TCP4* were studied and provided a novel insight into how miR319 regulates plant architecture.

Correlation analysis between differentially expressed miRNAs and their targets demonstrated that nutrition and metal deprivation, energy supply deficiency, senescence and *TEOSINTE BRANCHED1/CYCLOIDEA/PCF* (*TCPs*) contributed to the premature termination of shoot development in rod-like mutant. The work further elucidates the mechanism of miR319, miR164, miR2111, miR395, miR408, miR5654 and novel_mir_142 participate in the regulation of plant architecture.

Keywords: *Brassica napus*, microRNAs, plant architecture, shoot apical meristem, miR319

Results

1.A rod-like mutant displayed pleiotropic phenotypes

Compared to normal plants, the height of the rod-like mutant is significantly lower and the length of the silique layer is shorter, exhibiting a compact architecture (Fig. 1A–D). The flower buds died during the early flowering stage and exhibited premature termination of shoot development (Fig. 1E–H).

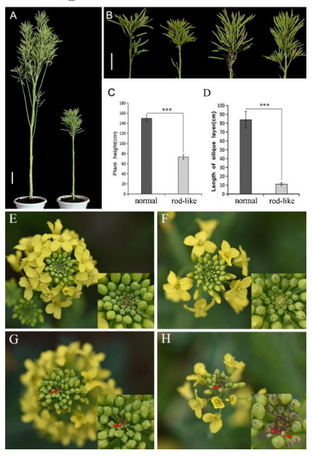

Fig. 1. Phenotypes of the rod-like and normal plants from the BC4F1 population.
(A).The whole plant architecture of the rod-like and normal plant. Scale bar=10cm. (B) Phenotypes of silique layer in rod-like plants. Scale bar=5cm. (C-D) Plant height (C) and the silique layer length (D) in the normal and rod-like plants. (E-H) The difference of the rod-like inflorescence compared to normal plants. The main (E) and lateral branch inflorescences (F) in normal plants with control. The main (G) and lateral branch inflorescences (H) in rod-like mutants. Error bars (C, D) represent standard deviation of samples from at least 20 plants. Statistical significance was assessed by Student's t-test (***P < 0.001). Magnification area of shoot apex showed in the right inset. Arrowheads indicate the abnormally dead buds.

2.Analysis of sRNA library sequencing

Four small RNA (sRNA) libraries from the shoot apex of normal and rod-like plants were sequenced (Table 1). A total of 925 non-redundant *B. napus* miRNA precursors were identified, representing 315 precursors for 74 known miRNAs and 610 precursors for 327 novel miRNAs. Unequal genomic or segmental duplications as well as tandem duplications of miRNAs might have greatly contributed to the miRNA expansion in *B. napus* (Fig. 2).

Table 1 Data set summary of four Small RNAs sequencing

Small RNAs	WT		Mutant	
	normal1	normal2	rod-like1	rod-like2
Total reads	13 057 499	13 085 047	14 230 591	14 230 797
Unique	5 056 175	5 039 670	5 371 861	5 390 887
Match genome	10 085 387(77.24%)	10 143 095(77.51%)	11 059 339(77.72%)	11 031 245(77.52%)

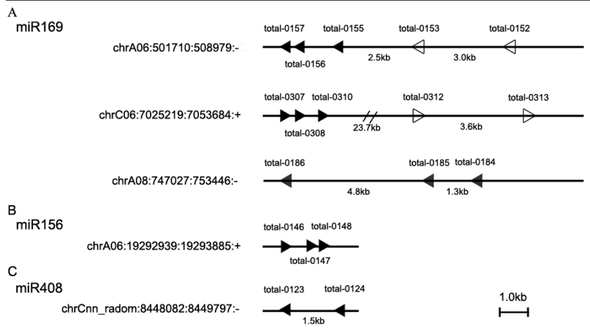

Fig. 2. Models to explain the tandem duplications of miRNAs occurred in *B. napus*.
(A) Two sub-genome analog and one sub-genome unique paralog clusters of miR169. (B, C) Sub-genome unique paralog clusters of miR156 (B) and miR408 (C).

3.Expression analysis of miRNAs in shoot apex

miRNA expression analysis identified 10 known miRNAs and 7 novel miRNAs that were differentially expressed between the two experiments. To confirm the expression of miRNAs identified by deep sequencing, the expression levels of 13 miRNAs were further analyzed (Fig. 3) .

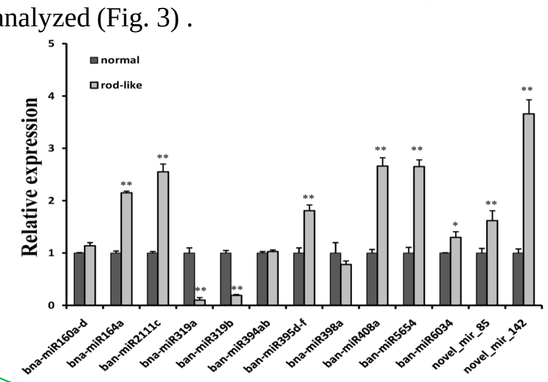

Fig. 3. Quantitative RT-PCR analyses of the abundance of twelve selected miRNAs in the shoot apex of normal and rod-like plants.
Statistical significance was assessed by Student's t-test (*P < 0.05; **P < 0.01).

4.Global identification of miRNA targets through degradome sequencing

Degradome sequencing identified 408 spliced transcripts, representing 264 targets for 25 known miRNA families and 144 targets of 58 novel miRNAs. To further evaluate our degradome results, 14 targets for a representative seven conserved and one novel miRNAs were tested using RLM-RACE (Fig. 4).

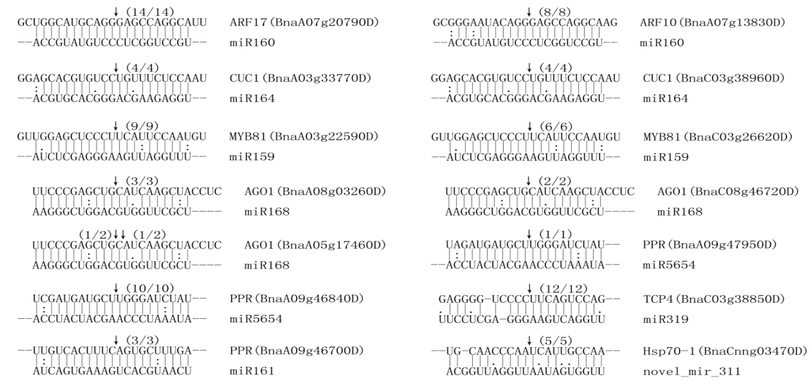

Fig. 4. Validation of predicted miRNA targets using RLM-RACE. The sequences depict the miRNA binding site within the target transcript.

5.Involvement of *TCP4* expression modulation in shoot meristem formation

In this study, we predicted two precursors (total-m0050 and total-m0101) of bna-miR319 that have not been previously identified in *B. napus*. Both precursors of bna-miR319 can form perfect secondary hairpin structures (Fig. 5A). qRT-PCR analysis revealed that when miR319 accumulated strongly in transgenic plants, the expression of its three target genes (At*TCP3*, At*TCP4*, and At*TCP10*) sharply decreased, implicating the activity of these two precursors in miRNA-target pair regulation (Fig. 5B). Moreover, the miR319 over-expressing transformed plants had cotyledon epinasty and serrated leaves with the typical feature of the jaw-D mutant that overexpresses ath-miR319a (Fig. 5C, D). we generated a cleavage-resistant vector (35S::m6*TCP4*) by introducing six silent mutations in the miR319 binding site (without changing the amino acid sequence) and transformed it into wild type Columbia (Col-0) plants (Fig. 5E). We determined *TCP4* transcript levels in 35::*m6TCP4* transgenic plants and observed a significant increase in expression in the mutant plants with respect to the wild-type Col-0 plants (Fig. 5F). The low-*TCP4* expressing lines had smaller leaves and exhibited a reduction in plant size (Fig. 5G), whereas high-*TCP4* expressing transgenic lines showed dramatic shoot meristem termination and slender leaves (Fig. 5H).

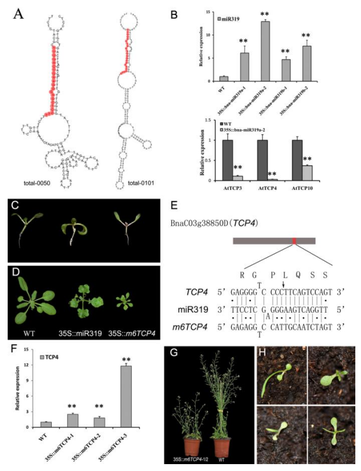

Fig. 5. Phenotypes of bna-miR319 and TCP4 over-expressed transgenic plants.
(A) The secondary hairpin structures of the two precursors of bna-miR319. (B) Relative expression of miR319 and its targets in transgenic lines, compared to WT. (C, D) one-week-old (C) and four-week-old (D) rosettes of Arabidopsis lines with increased bna-miR319 (35S::MIR319) and *TCP4* (35S::m6TCP4) compared to WT. (E) Gene structure of *TCP4* with the miR319 recognition site (red box) and the sequence of the miR319-resistant *m6TCP4*. Bases that differ from *TCP4* are indicated in red. (F) Relative expression of *TCP4* in 35S::m6TCP4 transgenic lines, compared to WT. (G) The plant architecture of 35S::m6TCP4 line with small increased *TCP4* transcript level and WT. (H) Different patterning defects in 35S::m6TCP4 seedlings transformed with a stronger increased *TCP4* transcript levels. Statistical significance was assessed by Student's t-test (*P < 0.05; **P < 0.01).

Conclusions

In summary, miRNAs are believed to function as novel intercellular signals in stem cells and to control the plant architecture. This study is the first to assess the miRNAs in shoot apex of *B. napus*. Our analysis of correlated expression between miRNAs and their target genes demonstrated that nutrient/metal deprivation and energy supply deficiency, senescence/premature, together with miR319/miR164, regulated the premature termination of shoot development (Fig. 6). For the miR2111, miR408 and miR395 might reflect a nutrition deficiency during shoot development, as nutrients and metals are critical for the whole plant type. In wheat, it has reported that tae-miR408 could affect heading time, plant height, leaf angle and other important agronomic traits. miR164 may affect the initiation of the axillary meristem and determines branch number; Overexpressing of os-miR164b resistant *OsNAC2* could increase rice yield and improve plant architecture. miR5654 might result in deficits in the energy supply on shoot development; Mitochondria may be abnormal in stem apex cells as PPR protein often binds to mitochondria transcripts. miR408 and novel_mir_142 may lead to a senescence/premature mechanism of shoot development; More significantly, the miR319 targeted *TCP4* should suppress meristem formation, resulting in premature termination of the SAM. TCPs act as negative regulators of cell dedifferentiation and suppress meristem formation *via* activation of miR164. Of these, we propose that miR319 regulated *TCP* transcription factors may help facilitate genetic engineering and molecular breeding of dicotyledonous plants for ideal plant architecture, as has been shown by the profound effect of miR156/miR529 in controlling expression of the *IPA1* gene in rice. Moreover, the function of the differentially expressed novel miRNAs will be further validated to explore the interactions of miRNAs, representing a novel and feasible approach to gain insight into the associated developmental mechanisms.

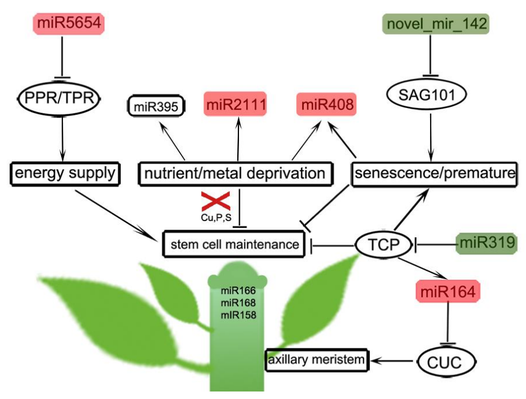

Fig. 6. A hypothetical model of the potential miRNA regulation network for plant architecture in rod-like mutant. The red rounded rectangles and green rounded rectangles represent the up-regulated and down-regulated miRNAs in the rod-like mutant, respectively. Arrows show simultaneous effect in the pathway while nail shape represents repression.